

adjacent to Q . The solution is indicated by the arrow in Fig. 9 and has a shape as given by curve b in Fig. 10. For comparison, the solution for low applied voltages as given in Fig. 8 and discussed before is pictured by curve a in Fig. 10.

With further increasing voltage, the solution comes closer to the singular point II, and hence the width of the high-field domain in R grows, as discussed in Sec. 2 for the homogeneous-excitation case. The electron density $n_s(E_T^*)$ controls the saturation current and therefore determines the electron density at the boundary between Q and R , which, in good approximation, is given by n_{II} (Fig. 9). Changing n_s by variation of the excitation in region Q changes n_{II} .

Using Eq. (4), $n_s(E)$ for different illuminations in region Q (see Fig. 11) is obtained from the measured current-voltage characteristics (some of which are given

in Fig. 4). In Fig. 11, $n_2(E)$ as determined by j is also drawn. This shows that E_{T^*} , i.e., the field in region Q , lies markedly below E_{II} (see also Fig. 10), in agreement with the discussion given above. Figure 11 also shows that the mobility is nearly field-independent up to at least 17 kV/cm (see curve 1). The decrease of $n_s(E)$ with field at lower-field values for stronger quenching (curves 2-7) can be explained by field-enhanced ionization of sensitizing centers. This and the general behavior of $n_1(E)$ will be discussed in more detail in a future paper.

ACKNOWLEDGMENTS

We would like to acknowledge the growing of the CdS platelets by L. van den Berg and the construction of the crystal holder by M. Weaver and E. E. Riley.

Infrared Spectral Emittance and Optical Properties of Yttrium Vanadate

H. E. RAST, H. H. CASPERS, AND S. A. MILLER

Infrared Division, Research Department, Naval Weapons Center Corona Laboratories
Corona, California 91720*

(Received 13 November 1967)

The infrared spectral emittance E of single crystals of YVO_4 has been examined near 4.2 and 77°K in the wavelength range 4–125 μ m. Of the expected seven active transverse optical modes at $\mathbf{k}\sim 0$, six have been observed and assigned to their symmetry species based on their polarization with respect to the crystalline axes. The observed frequencies of the transverse optic E_u modes were 196, 261, and 788 cm^{-1} ; and for A_{2u} modes, 310, 455, and 803 cm^{-1} . The relation between emittance and reflectance, $E=1-R$ in the opaque region of lattice vibrations, permits one to determine the reflectance R . By least-square-fitting the reflectance data to an independent set of damped harmonic oscillators, infrared dispersion parameters were determined for the E_u vibrations.

INTRODUCTION

RECENTLY, some interest has arisen in yttrium orthovanadate as a medium for spectroscopic studies of rare-earth ions and as a host material for lasers.¹⁻⁴ It is natural, therefore, to investigate the lattice vibrations of YVO_4 and to determine the optical properties and the extent to which the phonon spectrum might influence the spectral properties of doped rare-earth ions. In a previous report,⁵ the crystal structure of YVO_4 was analyzed group-theoretically to predict the expected $\mathbf{k}=0$ lattice vibrations, and the experi-

mental Raman spectrum was presented. In the work presented here, we examine the infrared spectrum of YVO_4 and correlate the observed data with the results of the Raman spectrum. Finally, the determination of the optical constants is discussed.

Lattice Vibrations of YVO_4

The crystal structure of YVO_4 is isomorphic to zircon, having space-group symmetry D_{4h} ¹⁹. Figure 1 depicts this tetragonal crystal structure and illustrates the primitive cell. With two molecules per primitive cell, this structure gives rise to 36 vibrational modes at $\mathbf{k}=0$, including crystal translations. The group-theoretical analysis of the lattice vibrations was carried out in great detail elsewhere⁵ and will not be repeated here. Instead, we summarize the results of that analysis in Table I by including the number, symmetry, and activity of the expected motions under D_{4h} symmetry. Only seven of these modes are infrared active: Three

* Formerly Naval Ordnance Laboratory, Corona, Calif.

¹ C. Brecher, H. Samelson, A. Lempicki, R. Riley, and T. Peters, *Phys. Rev.* **155**, 178 (1967).

² J. R. O'Connor, *Appl. Phys. Letters* **9**, 407 (1966).

³ W. Wanmaker, A. Brill, J. ter Vrugt, and J. Broos, *Philips Res. Rept.* **21**, 270 (1966).

⁴ A. K. Levine and F. C. Palilla, *Appl. Phys. Letters* **6**, 118 (1964).

⁵ S. A. Miller, H. H. Caspers, and H. E. Rast, *Phys. Rev.* **168**, 964 (1968).

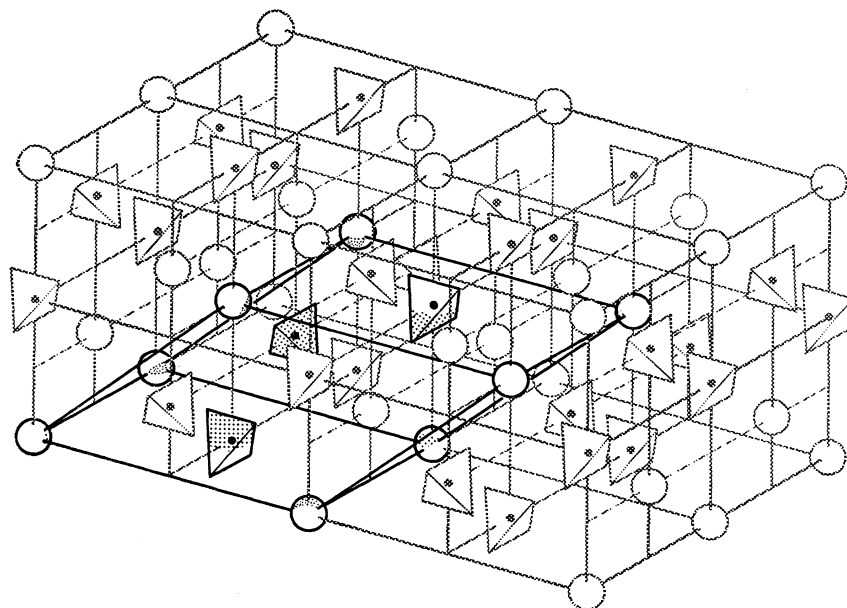


FIG. 1. Crystal structure of YVO_4 showing primitive cell. The VO_4^{-3} ions are represented by tetrahedra and balls indicate yttrium atoms.

belong to the A_{2u} representation of D_{4h} and are predicted to be polarized parallel to the crystalline c axis (z direction). The other four modes belong to the E_u representation and should appear as four doubly degenerate modes whose vibrational motions are in the x, y plane perpendicular to the crystalline c axis.

EXPERIMENTAL

Single crystals of yttrium orthovanadate were obtained from Vinor Laboratories. The crystals were oriented by x ray, cut, and polished. The crystals were prepared for examination in two ways. One sample was cut so it could be examined with the wave vector of the light parallel to the c axis (axial observation); the other sample was cut so the direction of light propagation was perpendicular to the optic axis of the crystal (transverse observation). The purpose here was to obtain spectra containing only those infrared transitions due to E_u modes (motion in the x, y plane perpendicular to the c axis) and additional spectra containing transitions due to all active infrared modes ($E_u + A_{2u}$). In this manner it is possible to assign observed transitions to their symmetry species.

The spectral emittance E is defined as the ratio of thermal radiation emitted per unit area by the sample to that emitted by a blackbody at the same temperature. If radiation is incident on a sample, it can be shown that the emittance, transmittance, and reflectance obey the relation⁶

$$E + R + T = 1, \quad (1)$$

if we define R and T as the fractions of incident radiation reflected and transmitted, respectively. The

experimental techniques involved in making measurements of E have been discussed by Stierwalt.^{7,8} In the spectral region of active optic mode frequencies, crystals are generally opaque, so Eq. (1) becomes

$$E + R = 1. \quad (2)$$

Therefore, a measurement of E at normal incidence is equivalent to a measurement of reflectance at normal incidence and one may analyze the reflection spectra by classical dispersion theory or Kramers-Kronig inversion.⁹

The spectral emittance of YVO_4 at 4.2 and 77°K was measured in the range 4–125 μm on the spectrophotometers modified by Stierwalt.^{7,8} In these measurements, the emittance is determined in a direction perpendicular or parallel to the optic axis of the crystal. Most measurements were made near 77°K, since there appeared to be little difference in the spectra compared to those at 4.2°K. A portion of the spectrum in the range 4–20 μm is shown in Fig. 2.

Infrared absorption measurements were made at room temperature in the spectral range 5–35 μm , utilizing a Perkin-Elmer Model 21 spectrophotometer and a Beckman IR-5 spectrophotometer. In these measurements, the crystal samples were oriented as in the emittance studies. However, in order to obtain reasonable transmission, it was necessary to cut and polish the crystals to a thickness on the order of 100 μm . The crystals were mounted on a polished disk of cesium bromide with paraffin and could be examined successively in decreasing thickness without removing the sample from the CsBr substrate.

⁷ D. L. Stierwalt, Appl. Opt. 5, 1911 (1966).

⁸ D. L. Stierwalt, J. Bernstein, and D. Kirk, Appl. Opt. 2, 1169 (1963).

⁹ D. H. Martin, Advan. Phys. 14, 39 (1965).

⁶ H. O. McMahon, J. Opt. Soc. Am. 40, 376 (1950).

TABLE I. Predicted $\mathbf{k} \sim 0$ modes of YVO_4 under D_{4h} symmetry with two molecules per primitive cell. Orientation of coordinate axes is with z parallel to the optic axis.

Species	Number	Activity	Polarization
A_{1g}	2	Raman	$\alpha_{xx}, \alpha_{yy}, \alpha_{zz}$
B_{1u}	2	Inactive	...
B_{1g}	1	Raman	α_{xx}, α_{yy}
A_{1u}	1	Inactive	...
A_{2g}	1	Inactive	...
B_{2u}	1	Inactive	...
B_{2g}	4	Raman	α_{xy}
A_{2u}	1	Inactive (acoustic)	...
	3	Infrared	z polarized
E_g	5	Raman	α_{zz}
E_u	1	Inactive (acoustic)	...
	4	Infrared	x, y polarized

RESULTS

The spectra revealed four distinct reflection bands for the electric vector perpendicular to the c axis. In the transverse observation, three additional bands appear along with the four x, y bands. Reference to Fig. 3, which is a portion of the spectrum in the range 19–46 μm , reveals two of these bands, one as a moderately intense reststrahlen at 310 cm^{-1} and a second very weak band at 455 cm^{-1} .

Since the E_u modes were predicted to be polarized perpendicular to the optic axis of the crystal, three reflection bands appearing in the axial observation have been assigned this symmetry. These bands have transverse optic frequencies of 196, 261, and 788 cm^{-1} . The x, y transition occurring at 310 cm^{-1} is somewhat weak and occurs as a satellite on the high-energy side of the band at 261 cm^{-1} . For reasons discussed later, it was not assigned as a fundamental.

The other crystal orientation reveals three additional bands at 310, 455, and 803 cm^{-1} which are distinctly absent in the axial spectra; these have been assigned as A_{2u} modes because such vibrations must occur with their dipole moments parallel to the optic axis. The A_{2u} mode at 803 cm^{-1} is observed in the transverse observation as an intense reststrahlen shifted toward higher energy away from the E_u mode at 788 cm^{-1} , although both bands overlap in this direction of observation. The transverse optic frequency of 803 cm^{-1}

TABLE II. Observed infrared transitions at 4.2 and 77°K and their symmetry assignments. The frequencies correspond to the $\mathbf{k} = 0$ transverse optic modes. z direction is parallel to the crystal-line c axis.

cm^{-1}	Assignment	Polarization
196	E_u	x, y
261	E_u	x, y
(310) ^a	(E_u) ^a	x, y
310	A_{2u}	z
455	A_{2u}	z
788	E_u	x, y
803	A_{2u}	z

^a Probably *not* a fundamental lattice vibration.

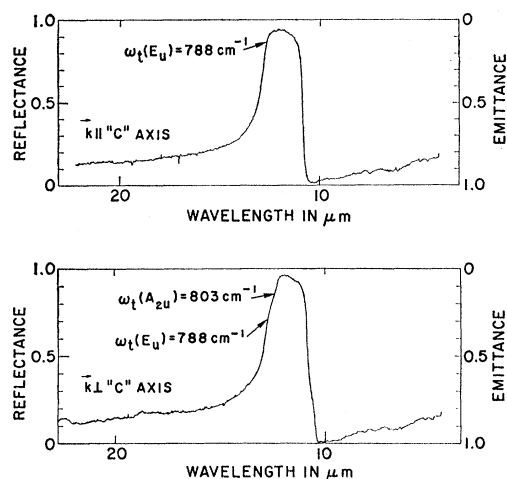


FIG. 2. Part of the emittance spectrum of YVO_4 near 77°K. Top: spectra obtained in axial observation showing E_u active mode only. Bottom: spectra obtained in transverse observation revealing E_u and A_{2u} active modes.

was determined from the low-frequency shoulder of the reststrahlen peak. This A_{2u} mode arises⁵ from the internal motions of the VO_4^{-3} cage and is degenerate with the E_u mode at 788 cm^{-1} , neglecting interaction between the two VO_4^{-3} ions in the primitive cell; in the crystal these degeneracies are lifted. The assignments are summarized in Table II.

The observation of the infrared absorption of thin crystal sections distinctly reveals the band at 455 cm^{-1} as a weak transition. There are good reasons, to be discussed shortly, for believing this transition is a fundamental. The remaining fundamentals were too intense to see through in absorption.

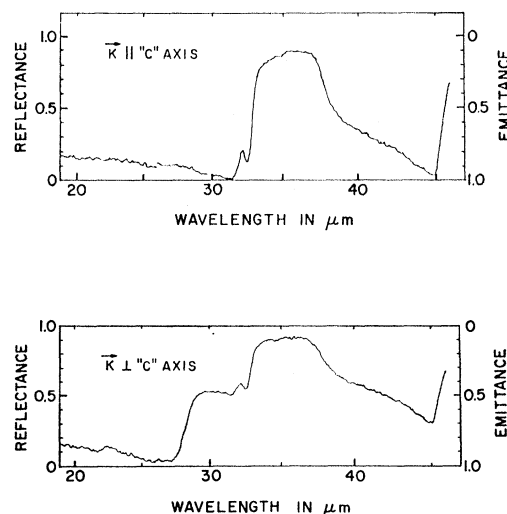


FIG. 3. Part of the emittance spectrum of YVO_4 near 77°K for different crystal orientations. Top: propagation parallel to optic axis. Bottom: propagation perpendicular to optic axis.

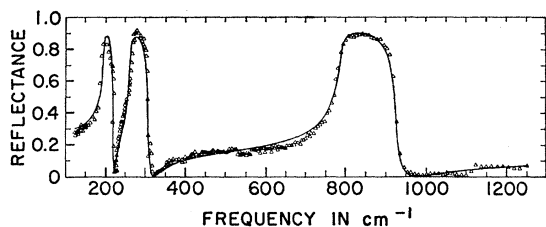


FIG. 4. Calculated and measured infrared reflectance spectrum of YVO_4 near 77°K . Direction of observation is parallel to the optic axis. Solid curve is calculated from classical dispersion theory. The points are experimental.

Dispersion Analysis

Infrared dispersion analysis was carried out on the reflection spectra observed with \mathbf{E} perpendicular to the optic axis. The four observed bands were fitted by least squares to the classical expression for the complex dielectric function,

$$\epsilon(\omega) = \epsilon_\infty + \sum_k \frac{4\pi\rho_k\omega_k^2}{\omega_k^2 - \omega^2 + i\gamma_k\omega},$$

where k runs over all the active E_u transverse optic

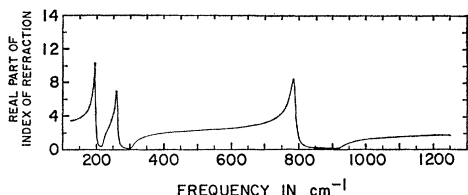


FIG. 5. Calculated real part of the refractive index of YVO_4 perpendicular to the optic axis.

modes. In the fitting process, the complex refractive index $N(\omega) = [\epsilon(\omega)]^{1/2}$ is used in the Fresnel formula for the normal incidence reflectance,

$$R = \frac{(N^* - 1)(N - 1)}{(N^* + 1)(N + 1)},$$

and the least-squares fitting is accomplished by the traditional method for nonlinear equations.¹⁰ The calculations were carried out in complex arithmetic on an IBM system 360/50 computer. In the input data, estimated values of the parameters, ω_i , $4\pi\rho_i$, and γ_i

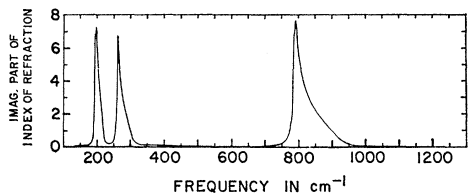


FIG. 6. Calculated imaginary part of the refractive index of YVO_4 perpendicular to the optic axis.

¹⁰ J. B. Scarborough, *Numerical Mathematical Analysis* (Johns Hopkins Press, Baltimore, 1955), 3rd ed., pp. 463-469.

were included and the calculations were iterated until the fit was self-consistent. The calculated and measured spectrum is presented for E_u modes in Fig. 4 and the dispersion parameters are given in Table III. The wave-number dependence of the calculated optical constants is plotted in Figs. 5-8. The very weak E_u band at 310 cm^{-1} was not included in the final fitting because it did not contribute significantly to the dielectric function. The value of γ listed in Table III

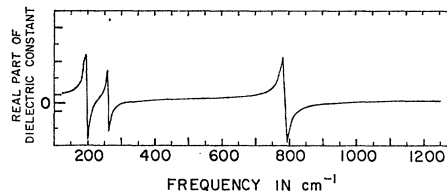


FIG. 7. Calculated real part of the dielectric function of YVO_4 perpendicular to the optic axis.

for this weak E_u mode was estimated making use of the fact that the inverse peak height of a reflection band is very nearly a linear function of (γ/ω_i) .^{11,12} The values of $4\pi\rho$ and ω_i for this band were estimated. The longitudinal frequencies of all other E_u modes were determined from the point where the positively increasing real part of the dielectric constant crosses zero. Values for the dispersion parameters for the $A_{2u}(z)$ modes were not determined because of the lack of polarized data which did not permit the separation of the A_{2u} and E_u modes in the transverse observation.

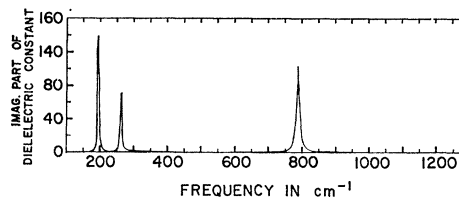


FIG. 8. Calculated imaginary part of the dielectric function of YVO_4 perpendicular to the optic axis.

DISCUSSION

The group-theoretical analysis of the YVO_4 crystal structure suggested that the motions of the atoms could be classified as "internal" or "external" according to whether or not the vibrations were analogous to those of the VO_4^{-3} complex. One should expect those frequencies of the VO_4^{-3} complex to be similar when the complex occurs in a crystal, while additional frequencies arise due to the motions of the VO_4^{-3} and Y^{+3} ions. This distinction is useful because it helps one to make vibrational assignments in crystals based on a knowledge of the symmetry assignments and observed fre-

¹¹ S. S. Mitra, in *Crystallography and Crystal Perfection*, edited by G. N. Ramachandran (Academic Press Inc., New York, 1963).

¹² S. S. Mitra, in *Progress in Infrared Spectroscopy*, edited by H. A. Szymanski (Plenum Press, Inc., New York, 1962), Vol. II.

TABLE III. Infrared dispersion parameters of YVO₄ for lattice vibrations perpendicular to crystalline *c* axis (*x*, *y*, or *E_u* modes). Data were taken at 77°K and least-squares fitted to a set of classical oscillators.

ω_{li} (cm ⁻¹)	196	261	310	788
ω_{ti} (cm ⁻¹)	219	307	(315)	926
$4\pi\rho_i$	2.78	1.43	(0.1)	1.39
γ_i/ω_{ti}	0.018	0.019	0.98	0.013
ϵ_∞	3.60±0.06	(measured at 6328 Å)		
ϵ_0	3.89	(calculated from least-squares fit)		
ϵ_0	9.59	(from $\epsilon_0 = \epsilon_\infty + \sum_i 4\pi\rho_i$)		
ϵ_0	9.58	(from LST relation ^a)		

^a Calculated from the generalized Lyddane-Sachs-Teller relation. See Refs. 14–16.

quencies of the free VO₄³⁻ complex. The vibrational frequencies of the VO₄³⁻ ion have been measured in solution by Siebert¹³ and occur at 870 (*A*₁), 345 (*E*), 825 (*F*₂), and 480 cm⁻¹ (*F*₂) where the letters in parentheses refer to the singly, doubly, and triply degenerate representations of the *T_d* group. Reference to Table IV shows how these representations split up under the reduced symmetry of the crystal and predicts that infrared-active crystal modes will arise from the two *F*₂ modes of the free VO₄³⁻ at 825 and 480 cm⁻¹. In making the reduction, however, we remember that there are two molecules per primitive cell so that the number of modes under *T_d* symmetry is doubled. These yield in the crystal a doubly degenerate *E_u* and a singly degenerate *A_{2u}* mode from the 825-cm⁻¹ vibrations. Likewise, the free complex vibrations at 480 cm⁻¹ split up into active *E_u* and *A_{2u}* modes. One now should expect to assign those frequencies in the crystal near 800 cm⁻¹ to the *A_{2u}* and *E_u* modes arising from the free complex and also those in the vicinity of 480 cm⁻¹. The assigned frequencies in the crystal spectra at 803 (*A_{2u}*), 788 (*E_u*), and 455 cm⁻¹ (*A_{2u}*) are consistent with this reasoning. The remaining weak mode at 310 cm⁻¹ (*E_u*) appears not to be a fundamental. It is possible, however, that the “internal” *E_u* mode is much weaker than the *A_{2u}* mode at 455 cm⁻¹ and was *not*

TABLE IV. Reduction of VO₄³⁻ modes from *T_d* to *D_{4h}* symmetry

<i>T_d</i> (free complex)	<i>D_{4h}</i> (crystal)	
(2 VO ₄ ³⁻)	(2 VO ₄ ³⁻)	
2 <i>A</i> ₁ (ν_1 —870 cm ⁻¹)	ν_1 (<i>A</i> _{1g}) ν_1 (<i>B</i> _{1u})	
2 <i>E</i> (ν_2 —345 cm ⁻¹)	ν_2 (<i>A</i> _{1g}) ν_2 (<i>B</i> _{1u}) ν_2 (<i>B</i> _{1g}) ν_2 (<i>A</i> _{1u})	
2 <i>F</i> ₂ (ν_3 —835 cm ⁻¹)	ν_3 (<i>B</i> _{2g}) ν_3 (<i>A</i> _{2u})	(IR-active)
	ν_3 (<i>E_g</i>) ν_3 (<i>E_u</i>)	(IR-active)
2 <i>F</i> ₂ (ν_4 —480 cm ⁻¹)	ν_4 (<i>B</i> _{2g}) ν_4 (<i>A</i> _{2u})	(IR-active)
	ν_4 (<i>E_g</i>) ν_4 (<i>E_u</i>)	(IR-active)

¹³ H. Siebert, Z. Anorg. Allgem. Chem. **275**, 225 (1954).

observed. One must then attribute the weak 310-cm⁻¹ band to anharmonic effects similar to the sidebands observed in other ionic crystals. Moreover, the fact that it appears on the high-energy side of the restrahlen peak associated with the 261-cm⁻¹ mode is consistent with this explanation. Examination of the symmetry coordinates⁵ for the infrared modes arising from the 480-cm⁻¹ frequency of the free VO₄³⁻ complex suggests a very small dipole moment associated with this vibration. The transverse orientation revealed a very weak *A_{2u}* mode at 455 cm⁻¹ in agreement with the small dipole moment predicted by examination of its symmetry coordinates.⁵ Based on the foregoing reasons we must conclude that the small *E_u* peak at 310 cm⁻¹ is probably a multiphonon combination and we have not observed one of the expected *E_u* modes arising from “internal” vibration of the free VO₄³⁻ complex which should have a frequency nearer to 480 cm⁻¹.

The remaining three transitions are “external” and must correspond as assigned here to the 196- (*E_u*), 261- (*E_u*), and 310-cm⁻¹ (*A_{2u}*) bands. Moreover, the frequencies are lower than the “internal” vibrations and consistent with the range of lattice frequencies generally observed for ionic crystals.

In the calculation of the optical constants for the *E_u* modes a reasonably good fit was obtained using a classical oscillator fit to the three intense reflection bands. The short-wavelength data indicate that the reflectance is approaching a limiting value of 0.10 from which one may estimate a value for the short-wavelength refractive index of 1.92. This is to be compared with the value of 1.86 measured at 6328 Å and the value of 1.97 determined from the classical oscillator fit. The zero-frequency dielectric constant was calculated from the generalized Lyddane-Sachs-Teller relation,^{14–16}

$$\frac{\epsilon_0}{\epsilon_\infty} = \prod_i \left\{ \frac{\omega_{li}}{\omega_{ti}} \right\}^2,$$

where ω_{li} and ω_{ti} are, respectively, the longitudinal and transverse optical frequencies at $\mathbf{k} \sim 0$. As indicated in Table III, the calculated value of 9.58 agrees well with the value 9.59 obtained from the oscillator sum rule

$$\epsilon_0 = \epsilon_\infty + \sum_i 4\pi\rho_i,$$

where the values of ϵ_∞ and $4\pi\rho_i$ were determined from the least-squares fit to a set of independent oscillators.

ACKNOWLEDGMENTS

We are grateful to D. L. Stierwalt and J. Bernstein for patiently taking the spectral emittance data. In addition, D. Smith kindly programmed the classical dispersion calculations.

¹⁴ W. Cochran, Z. Krist. **112**, 465 (1959).

¹⁵ T. Kurosawa, J. Phys. Soc. Japan **16**, 1298 (1961).

¹⁶ R. A. Satten, J. Chem. Phys. **41**, 281 (1964).